Cancer Immunology, Immunotherapy (2025) 74:180
https://doi.org/10.1007/s00262-025-04031-1

RESEARCH

USP5 motivates immunosuppressive microenvironment in multiple myeloma by activating STAT2-PFKFB4-mediated glycolysis

Shifeng Long[1] · Ting Ding[1] · Yongliang Zheng[1] · Jinmei Shao[1] · Yan Liu[2] · Qinglan Wang[2]

Received: 22 October 2024 / Accepted: 21 March 2025

Abstract

Background Glycolysis, a classic characteristic of cancer cells, can drive cancer progression by generating lactate, which play as a key immunosuppressive mediator. Currently, ubiquitin-specific proteases 5 (USP5) has been demonstrated to facilitate tumor cell survival in multiple myeloma (MM), whereas whether USP5 was involved in glycolysis-lactate production pathway and immunosuppressive microenvironment formation in MM remain unknown.

Methods The gene and protein expression characteristics were assessed via qRT-PCR and western blot. MM cell survival was determined by CCK-8 and flow cytometry analysis. Glycolysis was evaluated by examining glucose uptake, lactate production and ATP level via corresponding kits. Tumor-associated macrophages polarization was tested via measurement of M1/M2-like macrophage markers using qRT-PCR and flow cytometry methods. Dual-luciferase reporter, chromatin immunoprecipitation and co-immunoprecipitation assays were conducted to verified molecular relationship. Xenograft model was used for verified cellular findings.

Results USP5 was abnormally overexpressed in MM patients and cell lines. Knockdown of USP5 could restrain MM cell survival and glycolysis activity, thus reducing lactate-mediated immunosuppressive M2-like macrophage polarization in vitro and in vivo, whereas overexpression of USP5 play opposite impacts. Mechanistically, USP5 could downregulate the ubiquitination modification of STAT to stabilize STAT2 protein, thus activating PFKFB4 transcription. Moreover, STAT2 could overturn the regulatory role of USP5 on MM cell survival, glycolysis and lactate-mediated immunosuppressive M2-like macrophage polarization.

Conclusion These findings elucidated that USP5 served as a regulator of glycolysis-lactate to stimulate M2-like macrophage formation by regulating STAT2-PFKFB4 signaling, which supported that USP5 could be a viable therapeutic target of MM treatment.

Keywords Multiple myeloma · Glycolysis · Macrophage polarization · USP5

Introduction

Multiple myeloma (MM) is a highly heterogeneous hematological malignancy characterized by its high recurrence rate and difficulty in achieving a cure. In 2019, there were 155,688 new cases of MM reported globally, with an age-standardized incidence rate of 1.92 per 100,000 individuals [1]. Studies have shown that the development of MM is a multistep process involving genetic alterations in tumor cells and changes within the bone marrow microenvironment [2]. Cellular components of the bone marrow microenvironment, such as macrophages, immune T cells, stromal cells, osteoclasts, and myeloid-derived suppressor cells, interact with malignant plasma cells in MM [3, 4]. Among these, the malignant proliferation of MM cells promotes the formation of an immunosuppressive bone marrow microenvironment (BMME), which in turn provides a favorable niche for MM cell survival and proliferation while protecting MM cells from drug toxicity [5, 6]. Therefore, investigating the mechanisms of interaction between MM cells and the

✉ Shifeng Long
longshifeng1910@163.com

[1] Department of Hematology, The Affiliated Hospital of Jinggangshan University, Ji'an 343000, Jiangxi Province, People's Republic of China

[2] Department of Transfusion Medicine, The Affiliated Hospital of Jinggangshan University, Ji'an 343000, Jiangxi Province, People's Republic of China

Published online: 24 April 2025

microenvironment is significant for elucidating the mechanisms of MM development, early diagnosis, and treatment.

Warburg effect is a key characteristic of tumor cells [7], playing a crucial role in tumor growth, metastasis, and immune tolerance [8, 9]. Growing evidence indicates that MM cells possess multiple metabolic features, including enhanced glycolysis and increased lactate production induced by upregulation of glucose transporters [10]. Metabolic disorders and the accumulation of metabolic products in MM cells are significant contributors to alterations in the BMME and dysfunction of immune cells within the BMME [11, 12]. Lactate, once considered merely a "metabolic waste" product of glycolysis, has been shown to be significantly elevated in tumor tissues compared to normal tissues. It can act as an immunomodulatory substance affecting the effector functions of innate and adaptive immune cells. During tumor development, disruption of lactate homeostasis leads to acidosis, angiogenesis, immunosuppression, tumor cell proliferation, and survival, promoting the formation of a tumor-immunosuppressive microenvironment [13, 14]. It has been reported that tumor-derived lactate can induce tumor-associated macrophages (TAMs) toward M2-like macrophage polarization [15–17], and suppress T-cell cytotoxicity [18]. However, the mechanisms of glycolysis and lactate production in MM cells and their impact on macrophages within the BMME remain underreported.

Ubiquitin-specific proteases (USPs) are a class of enzymes that reverse protein ubiquitination, playing a crucial role in cellular activities such as signal transduction, DNA damage repair, and cell cycle regulation by controlling protein stability and function. USP5, a member of the USP family, exhibits different expression patterns and functional characteristics across various types of cancer, making it an important molecule in tumor biology research [19]. In MM, knockdown of USP5 can suppress MM cell proliferation and survival, inducing apoptosis [20–22], suggesting that USP5 may be a key factor in promoting MM development. Besides, a recent study has shown that USP5 can activate aerobic glycolysis and promote the progression of triple-negative breast cancer by deubiquitinating and stabilizing PFKP [23]. Similarly, USP5 promotes hepatocellular carcinoma progression by reprogramming glucose metabolism [24]. This indicates that USP5 may play a significant role in the glycolysis of tumor cells. However, whether USP5 regulates glycolysis in MM cells to participate in the formation of the tumor-immunosuppressive microenvironment remains to be investigated.

In this work, we planned to elucidate the underlying role and mechanism of USP5 in regulating glycolysis and immunosuppressive microenvironment in MM. Our findings reported that USP5 was abnormally overexpressed in MM patients, and knockdown of USP5 greatly impaired the survival and glycolysis, reduced lactate production, thus repressing immunosuppressive macrophages formation, while overexpression USP5 exhibited opposite roles. Mechanistically, USP5 could stabilize STAT2 xUSP5 on MM progression and immunosuppressive microenvironment and provided a potential antitumor therapy of MM by inhibiting USP5 deubiquitination activities.

Materials and methods

Clinical sample collection

A total of 20 healthy bone marrow (BM) donors and 38 MM patients diagnosed in The Affiliated Hospital of Jinggangshan University were enrolled in this work. Briefly, the BM stromal cells (BMSCs) were isolated form BM samples of all participants as described previously [25]. Subsequently, the mononuclear cells were subsequently isolated via gradient density centrifugation followed by purification of the primary myeloma cells using CD138-coated magnetic beads (Miltenyi Biotech, Bergisch Gladbach, Germany). The collection and use of clinical specimens were approved by the ethics committee of The Affiliated Hospital of Jinggangshan University and performed in accordance with the Declaration of Helsinki. All subjects were provided written informed consent.

Cell culture and administration

The normal plasma cell line (nPCs) was sourced from Fenghui Biotechnology Co., Ltd (Changsha, China), and MM cell lines including MM.1S, U266 and NCI-H929 were procured from the American Type Culture Collection (ATCC) (Manassas, Virginia, USA). INA-6, a human IL-6-dependent cell line, was provided previously by Gramatzki group (Kiel, Germany). These cells were maintained in RPMI-1640 medium (Invitrogen, Carlsbad, CA, USA) enriched with 10% fetal bovine serum (FBS, Gibco, Grand Island, NY, USA), alongside 1% penicillin–streptomycin. The medium of INA-6 cells was extra added recombinant human IL-6 (1 ng/ml, Merck Millipore, Billerica, MA, USA). Cells were cultivated under a controlled environment set at 37 °C and 5% CO_2. To block lactate production, MM cells were exposed in complete medium containing 25 μM oxamic acid sodium (OXM, MedChemExpress, Monmouth Junction, NJ, USA) administration for 48 h. For hypoxic induction, all MM cell lines were maintained in 1% O_2, 94% N_2 and 5% CO_2 condition for 48 h. For stromal cell co-culture, BM stromal cells were co-cultured with MM cell lines by using a transwell chamber (Sigma-Aldrich, St Louis, MO, USA) at a ratio of 1:5 for 48 h.

Cell transfection

The short hairpin RNA against USP5 and STAT2, overexpressing vectors of USP5 and STAT2, as well as their negative controls were all sourced from GenePharma (Suzhou, China). For cell transfection, MM cells were pre-plated into six-well plate, and when cell growth reached to ~ 80% confluences, the above nucleotides were transfected into cells by using Lipofectamine 3000 (Invitrogen, Carlsbad, CA, USA), respectively. After 48 h, cells were obtained for determining the transfection efficiency.

Quantitative Real Time-PCR (qRT-PCR) assay

The total RNA was extracted utilizing TRIzol Reagent (Invitrogen). The PrimScript RT kit (Takara, Dalian, China) was applied to generate cDNA. Subsequently, qRT-PCR was performed according to the instructions of PrimeScript RT Master Mix kit (Takara). The RNA transcripts were analyzed according to $2^{-\Delta\Delta Ct}$ method. GAPDH was used as the internal gene. The primer sequences are provided in Table 1.

Western blot

The antibodies used in this experiment were listed as follows: anti-USP5 (ab154170), anti-signal transducer and activator of transcription 2 (STAT2, ab32367), anti-p-STAT2 (Y690) (ab191601), anti-6-Phosphofructose-2-kinase/fructose-2,6-bisphosphatase 4 (PFKFB4, ab318193), anti-HA (ab9110), anti-GAPDH (ab8245), and anti-β-actin (ab8226). All of them were obtained from Abcam company (Cambridge, USA). For western blot assay, the total proteins were extracted by using RIPA buffer (Cell Signal Technology, MA, USA). BCA kit (Beyotime, Shanghai, China) quantified the protein concentration. Then, 20 μg proteins were loading to perform 10% SDS-PAGE, and moved on PVDF membranes (Millipore, MA). After blocking, the primary antibodies were incubated with the members at 4℃ for overnight. Subsequently, the goat anti-rabbit IgG H&L (HRP) (ab6721) was further incubated with the membranes for 1 h. ECL detection system (Thermo Fisher Scientific, Wilmington, DE, USA) stained the membranes, and further quantified by ImageJ software.

Cell survival detection

A Commercial cell counting kit-8 (CCK-8) was acquired from KeyGEN (Nanjing, China) for determining cell viability. In a 96-well plate, cells were seeded at a density of 5×10^3/well for cultivation 24 h. Then, 10 μL of CCK-8 regent was added and following reaction for 4 h. Finally, the OD value at 450 nm was recorded through a microplate reader (Thermo Fisher Scientific).

Apoptosis detection

Annexin V-FITC/PI staining kit (Thermo Fisher Scientific) was used to assess cell apoptosis. After different treatment, the cells were centrifuged and collected and washed with pre-cooled PBS regent. Then, 100 μL cell suspension (1×10^6 cells/mL) were stained by a reaction containing propidium iodide (PI, 10 μL) and Annexin V-FITC (5 μL) at room temperature/dark environment for 10 min. Finally, cell apoptosis was quantified by flow cytometry (BD Biosciences, San Jose, CA, USA).

Glucose uptake, lactate production and ATP detection

The glycolysis of MM cells was determined by assessing the level of glucose uptake, lactic acid production and ATP level. After indicated treatment, cells were collected and the

Table 1 Primer sequences in qRT-PCR

Gene	Forward (5′-3′)	Reverse (5′-3′)
USP5	ACGTTTCTGGGCTTTGGGAA	CTGTAGCAGGGTCCTCCTCT
HK2	GATTTCACCAAGCGTGGACT	GTCGTCACAGGTGCTCTCAA
PFKP	TGCAGCAGAGGATGGGATTG	CCCTCCAGTCACCCCTTACA
PKM2	ATGAGTACCATGCGGAGACC	AGTCCAGCCACAGGATGTTC
Arg1	CCCTTTGCTGACATCCCTAA	GACTCCAAGATCAGGGTGGA
CD206	ACTAGGCAATGCCAATGGAG	TGGTCAGCGGGTCTTTATTC
IL-10	GCCAAGCCTTGTCTGAGATG	GGCCTTGCTCTTGTTTTCAC
TNF-α	GGCCTTGCTCTTGTTTTCAC	TGAGGTACAGGCCCTCTGAT
iNOS	CAGCATGTACCCTCGGTTCT	GGGGATCTGAATGTGCTGTT
IL-1β	CGATGCACCTGTACGATCAC	TCTTTCAACACGCAGGACAG
STAT2	ATTCTGCCGGGACATTCAGG	TCTGATGGGGGTCCAGAGAG
PFKFB4	CCCACGGGAATTGACACAGA	AGGCCCACCATGACAATGAG
GAPDH	CCAGGTGGTCTCCTCTGA	GCTGTAGCCAAATCGTTGT

cell supernatant was harvested, and the glucose, lactate and ATP levels were examined by Glucose Uptake Colorimetric Assay Kit (Biovision, Milpitas, CA, USA), Lactate Colorimetric Assay kit (Biovision) and ATP Colorimetric Assay kit t (Biovision) in line with the kit protocol accordingly.

Macrophage polarization measurement

Peripheral blood mononuclear cells (PBMCs) were obtained from healthy donors using a Ficoll-Hypaque (Ficoll® 400, Sigma-Aldrich) density gradient. Monocytes were subsequently isolated from the PBMCs with Human CD14 MicroBeads (Miltenyi Biotec, USA), following the manufacturer's instructions. The isolated monocytes were then cultured for 7 days in RPMI-1640 medium supplemented with 10% fetal bovine serum (FBS) and 100 ng/mL macrophage colony-stimulating factor (M-CSF) to differentiate into M0 macrophages. After indicated treatment, the cell supernatant of tumor cells from each group were centrifuged (1000 rpm, 10 min) and passed through 0.2 mm filters to obtain tumor-conditioned medium (TCM). Then, macrophages were maintained with 50% TCM plus 50% complete medium for two days. Next, macrophages were collected and washed twice with PBS, and followed by incubated with FITC-conjugated CD206 antibody (ab270647) for overnight. Finally, cells were analyzed by flow cytometry (BD Biosciences).

Co-Immunoprecipitation

MM cells were lysed in NP40 lysis buffer (Sigma-Aldrich) to harvest cell lysates. The specific antibody against USP5 (ab241311, Abcam) or IgG (ab172730, Abcam) were incubated with protein A/G agarose (Thermo Fisher Scientific) for overnight at 4 °C. Then, cell lysates were centrifuged (12000 rpm, 10 min) and followed by incubated with antibody-beads complex another for 12 h. Afterward, beads were washed five times and the precipitated proteins were eluted and further examined via western blot analysis.

Ubiquitination assays

The recombinant HA-ubiquitin, Flag-STAT2 and Flag-USP5 plasmids were acquired from GenePharma (Suzhou, China). The HA-ubiquitin and Flag-STAT2 plasmids were introduced into NCI-H929 cells which stably transfected with shNC or shUSP5. MM.1S cells were transfected with HA-ubiquitin alone or co-transfected with HA-ubiquitin and Flag-USP5. At 24-h post-transfection, cells were administrated with 10 μM MG132 (Sigma-Aldrich) for additional 8 h. The specific antibodies against STAT2 (ab280900, Abcam), Flag (ab205606, Abcam) were incubated with protein A/G agarose (Thermo Fisher Scientific) for overnight at 4℃. Next, cell lysates were incubated with the above antibody-beads complex another for 12 h. Thereafter, the resultants were washed five times, and precipitated proteins were eluted and subjected to western blot analysis.

Chromatin immunoprecipitation (ChIP)

To examine the transcriptional correlation between STAT2 and PFKFB4 promoter, MM cells were cross-linked with 1% formaldehyde for 10 min, and followed by adding glycine (final concentration at 0.125 M) to quenched cross-linking reaction. Then, cells were then washed with pre-cold PBS and lysed, and subjected to sonication to generate DNA fragment ranging from 100 to 500 bp. Specific STAT2 antibody (ab191601, Abcam) or IgG antibody (ab172730, Abcam) were pre-incubated with protein A agarose beads (Thermo Fisher Scientific), and followed by adding into cell lysates for overnight. Then, beads were collected and precipitated DNA fragments were extracted and subjected to qRT-PCR analysis.

Dual-luciferase assay

The amplified promoter fragment of PFKFB4 gene was inserted into the firefly plasmids in the pGL3-basic vectors (Promega, Madision, WI, USA). Then, NCI-H929 cells were introduced with 10 nM of shNC or shSTAT2 and 40 ng recombinant luciferase plasmids, and MM.1S cells were transfected with 10 nM of pcDNA3.1 or pcDNA3.1-STAT2 and 40 ng recombinant luciferase plasmids. After transfection for 48 h, luciferase activity was determined by utilizing dual-luciferase reporter assay system kit (Promega).

Xenograft experiments

Six-week-old BALB/c nude mice were brought from Hunan SJA Laboratory Animal Co., Ltd (Changsha, Hunan, China). THP-1 cells were sourced from ATCC and cultured in complete RPMI-1640 medium (Invitrogen). Before experiments, THP-1 cells were pre-stimulated with 100 ng/mL PMA (Sigma-Aldrich, St Louis, MO, USA) for 24 h to obtain M0 macrophages. NCI-H929 cells stably expressed shNC or shUSP5 were mixed with THP-1-derived macrophages at the ratio of 1:1. A xenograft tumor model was established via the subcutaneous injection into mice with the above cell suspension. Each group consisted of five mice. Tumor volume ($\text{length} \times \text{width}^2 \times 0.5$) was measured every four days starting eight days post-injection. After 28 days, the tumors were excised from the euthanized mice and their weights were recorded. This animal experiment was approved by the Animal Ethics Committee of The Affiliated Hospital of Jinggangshan University.

Immunofluorescence co-localization

Tumor tissues harvested from xenograft nude mice were fixed overnight in 4% formaldehyde, dehydrated, and embedded in paraffin. The embedded tissues were then sectioned into 5-μm-thick slices. Following this, the sections underwent deparaffinization and rehydration, followed by antigen retrieval and serum blocking. The primary antibodies of anti-CD11b (ab8878, Abcam) and anti-CD206 (ab64693) were added and incubated with the sections at 4 °C. Next day, the sections were washed and incubated with Alexa Fluor 488-labeled goat anti-rabbit IgG (ab150077, Abcam) for 1 h. Finally, the sections were incubated for 10 min with 4′,6-diamidino 2-phenylindole (DAPI, Beyotime) to stain the nucleus. Fluorescent microscopic images were captured and processed using a microscope (Nikon, Tokyo, Japan).

Data analysis

Results were repeated more than 3 times and expressed as "mean ± SD." GraphPad Prism 5.0 software was used for data statistical analysis. ANOVA or Student's t test were used for data comparison in multiple-group differences or two-group differences, respectively. $P < 0.05$ indicated the data were significant.

Results

USP5 was abnormally enhanced in MM patients and cell lines

The expression characteristic of USP5 in BM samples of MM patients and normal donors was determined, and the primary myeloma cells were purified to examine the expression pattern of USP5. As displayed in Fig. 1A, B, the expression of USP5 at mRNA and protein level were all greatly increased in MM patients than normal donors. Consistently, relative to nPCs, USP5 also exhibited a higher level in MM cell lines including MM.1S, U266, NCI-HP29 and INA-6 cells (Fig. 1C, D). As is well known, hypoxia is a significant characteristic of the MM microenvironment. Here, MM cell lines were exposed to hypoxic induction and co-cultured with BM stroll cells for 48 h, respectively. The results demonstrated that hypoxic induction and co-cultured with BM stroll cells remarkably upregulated USP5 mRNA and protein level (Fig. 1E–H). These results illustrated that USP5 was enriched in MM.

USP5 conferred the proliferation, apoptosis and glycolysis of MM cells in vitro

To probe the exact role of USP5 in MM cells, we knocked down USP5 expression in NCI-H929, INA-6 and U266 cells by transfection with shUSP5 and overexpressed USP5 expression in MM.1S cells through transfection with pcDNA3.1-USP5 plasmids. As confirmed by qRT-PCR analysis, shUSP5 transfection remarkably repressed USP5 expression in NCI-H929, INA-6 and U266 cells relative shNC transfection, and pcDNA3.1-USP5 strikingly enhanced USP5 expression in MM.1S cells than pcDNA3.1 transfection (Fig. 2A–C, Fig. S2A–C). Next, CCK-8 and flow cytometry analysis demonstrated that USP5 reduction obviously repressed cell viability and induced apoptosis in NCI-H929, INA-6 and U266 cells, and USP5 upregulation aggravated cell viability and repressed cell apoptosis of MM.1S cells (Fig. 2D, E, Fig. S2D, E). Besides, knockdown of USP5 downregulated the mRNA levels of glycolysis-related genes (HK2, PFKP, PKM2) in NCI-H929, INA-6 and U266 cells, while USP5 overexpression play opposite roles in MM.1S cells (Fig. 2F, Fig. S2F). Similarly, USP5 knockdown greatly inhibited glucose uptake, lactate generation and ATP content in NCI-H929 cells, and elevation of USP5 obviously restrained these changes in MM.1S cells (Fig. 2G–I, Fig. S2G–I). Overall, these changes indicated that USP5 boosted cell survival and glycolysis of MM cells.

USP5-induced immunosuppressive macrophage formation by regulating glycolysis-lactate pathway

Giving the consideration that increased glycolysis could induce tumor microenvironment acidification through the production of lactate [26]. Therefore, we further analyzed whether USP5 could modulate macrophage polarization by regulating glycolysis and lactate production. OXM, a specific LDH-A inhibitor, could block lactate generation [16]. As shown in Fig. 3A and Fig. S3A, the inhibitory role of USP5 knockdown on lactate production in NCI-H929, INA-6 and U2666 cells was aggravated by OXM co-treatment, while the promoting role of USP5 overexpression in MM.1S cells was overturned by OXM. Then, PBMCs-derived macrophages were co-cultured with TCM for 48 h. Afterward, macrophages were harvested and subjected to qRT-PCR assay. The results showed that USP5 downregulation markedly inhibited M2-like macrophage marker (Arg1, CD206, IL-10) expressions, and these changes were further strengthened by OXM (Fig. 3B, Fig. S3B). Inversely, increase in USP5 enhanced M2-like macrophage markers (Arg1, CD206, IL-10) expression, but these impacts were overturned by OXM (Fig. 3B), whereas alterations in M1 TAM markers such as TNF-α, iNOS and IL-1β were not evident (Fig. 3C, Fig. S3C). Flow cytometry analysis further identified that relative to control group, the reduction in USP5 silence on CD206-positive cell rate were intensified by OXM, and the promoting role of USP5 overexpression on

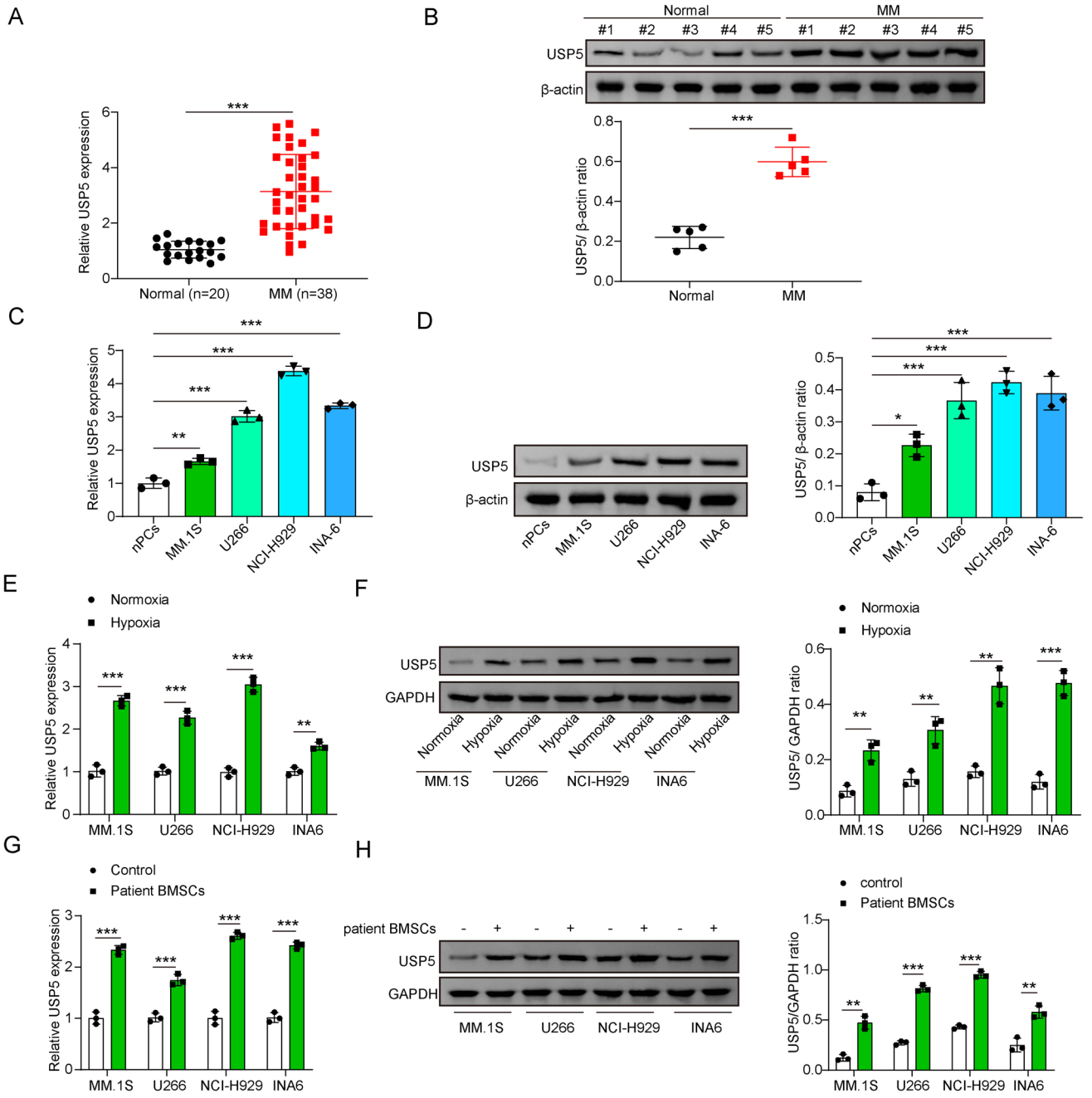

Fig. 1 USP5 was overexpressed in MM patients and MM cell lines. **A**, **B** The primary myeloma cells were isolated from BM samples of MM patients ($n=38$) and normal donors ($n=20$), and the characteristic of USP5 was determined via qRT-PCR and Western blot. **C**, **D** The mRNA and protein level of USP5 in nPCs and MM cell lines (MM.1S, U266, NCI-H929 and INA-6) were identified by qRT-PCR and Western blot, respectively. **E**, **F** MM cell lines (MM.1S, U266, NCI-H929 and INA-6) were exposed to normoxic and hypoxic condition for 48 h. Then, the mRNA and protein level of USP5 were evidenced by qRT-PCR and Western blot. **G**, **H** BM stromal cells were co-cultured with MM cells for 48 h, and the mRNA and protein level of USP5 were determined by qRT-PCR and Western blot. * $P<0.05$, ** $P<0.01$, *** $P<0.001$

CD206 cell rate was reversed by OXM (Fig. 3D, Fig. S3D). These results elucidated that USP5-induced glycolysis led to M2-like macrophages by lactate production.

USP5 stabilized STAT2 protein via *promoting its deubiquitylation*

Through prediction by Ubibrowser 2.0 database, the deubiquitylation modification site of USP5 on STAT2 protein is

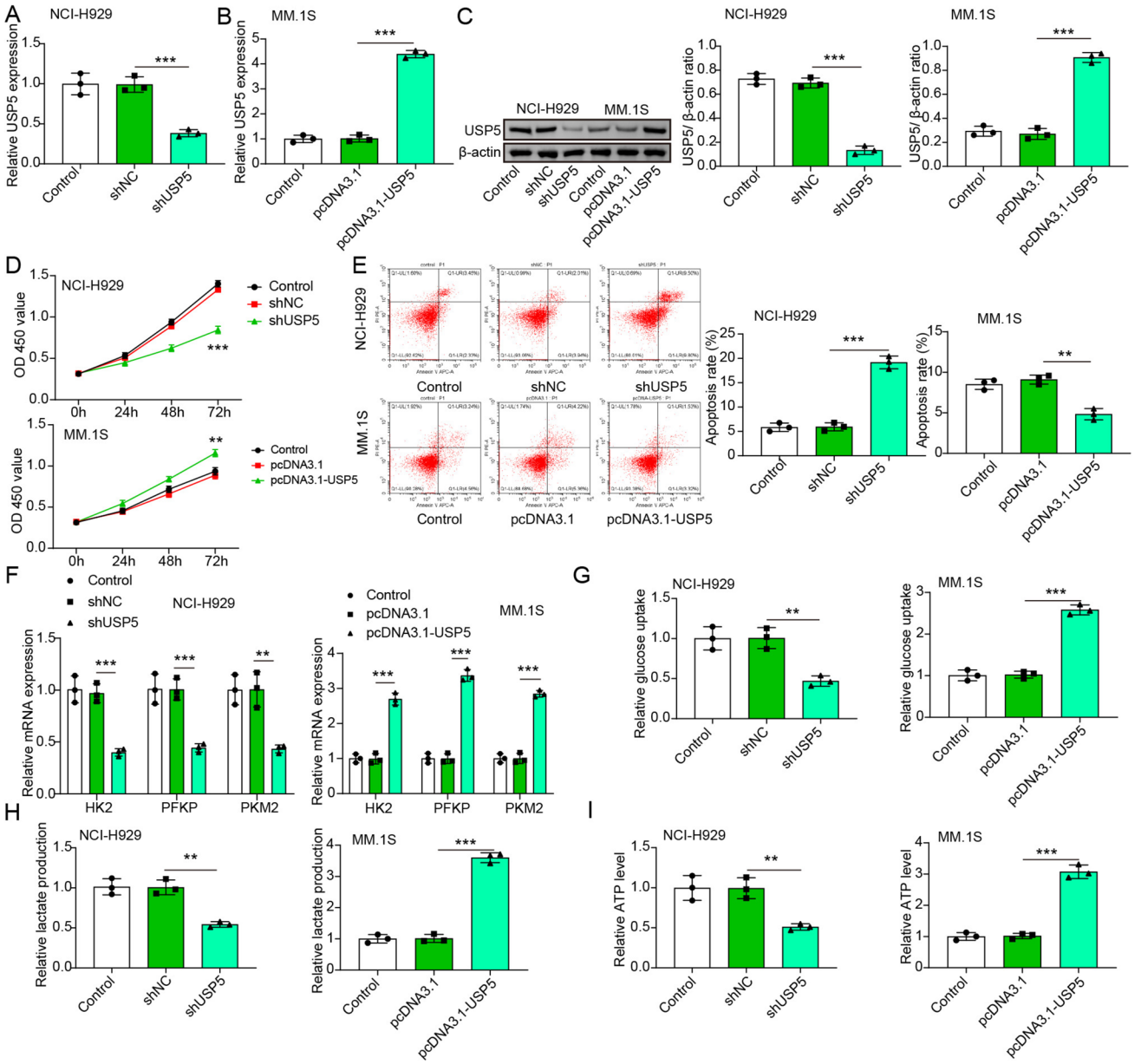

Fig. 2 USP5 conferred the proliferation, apoptosis and glycolysis of MM cells in vitro. NCI-H929 cells were transfected shNC or shUSP5, while MM.1S cells were transfected pcDNA3.1 or pcDNA3.1-USP5. After 48 h, the transfected cells were harvested for next experiments. **A**–**C** qRT-PCR and western blot were employed to examine the mRNA and protein levels of USP5. **D** Cell viability was quantified via CCK-8. **E** The apoptotic rate was evaluated by flow cytometry. **F** Glycolysis-associated genes including HK2, PFKP and PKM2 were assessed by qRT-PCR. **G**–**I** The glucose uptake, lactate production and ATP level were measured by corresponding kits. * $P<0.05$, ** $P<0.01$, *** $P<0.001$

displayed in Fig. 4A. Next, we confirmed that both overexpression and knockdown of USP5 had no significant effect on STAT2 mRNA levels (Fig. 4B, Fig. S4A). Whereas overexpression of USP5 elevated STAT2 and p-STAT2 (Y690) protein levels in MM.1S cells, USP5 silence downregulated STAT2 and p-STAT2 (Y690) protein levels (Fig. 4C, Fig. S1, Fig. S4B). Co-IP experiments further verified the direct interaction between STAT2 and USP5 (Fig. 4D, Fig. S4C). After CHX treatment, the repression of USP5 accelerated STAT2 protein degradation in NCI-H929 cells, and augmentation of USP5 delayed STAT2 protein degradation in MM.1S cells (Fig. 4E). The results of the in vitro ubiquitination experiment revealed that USP5 depletion enhanced the ubiquitination level of STAT2 in NCI-H929, INA-6 and U266 cells, and upregulation of USP5 decreased the ubiquitination level of STAT2 in MM.1S cells (Fig. 4F,

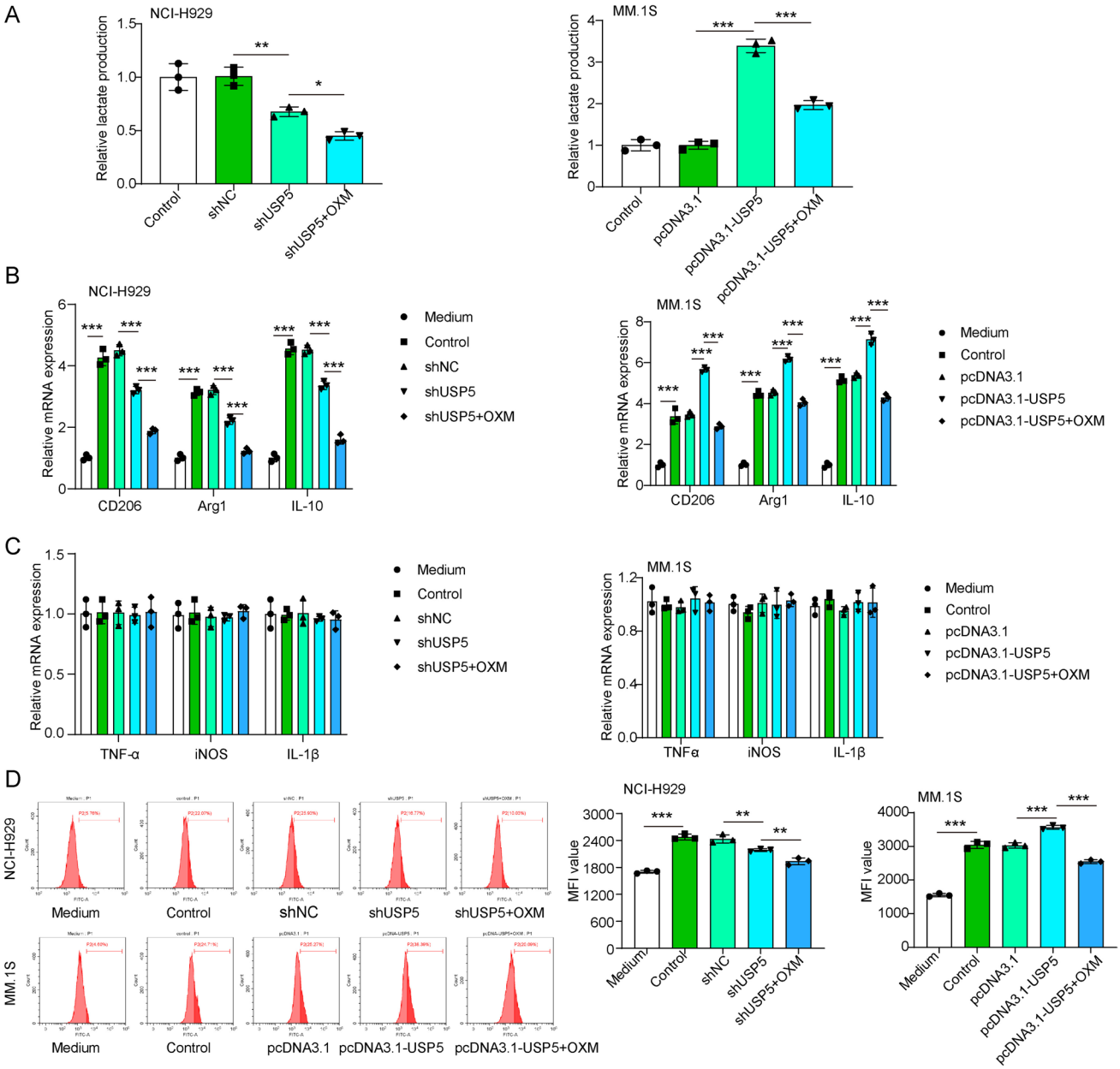

Fig. 3 USP5 conferred the proliferation, apoptosis and glycolysis of MM cells in vitro. The shUSP5 were co-treated with OXM into NCI-H929 cells, and pcDNA3.1-USP5 was co-treated with OXM into MM.1S cells. After 48 h, the treated cells were harvested for next experiments. **A** The lactate production of NCI-H929 and MM.1S cells was measured by commercial kit. The TCM of each group tumor cells were harvested and incubated with PBMCs-derived macrophages for 48 h. **B**, **C** qRT-PCR was employed for measuring M1-like macrophage markers (TNF-α, iNOS, IL-1β) and M2-like macrophage markers (Arg1, CD206, IL-10). **D** Flow cytometry analysis was used for determining CD206-positive macrophage rate. * $P < 0.05$, ** $P < 0.01$, *** $P < 0.001$

Fig. S4D). These findings showed that STAT2 was a direct ubiquitination modification target of USP5 in MM.

STAT2 activated PFKFB4 transcription

As indicated in Fig. 5A, Jaspar database showed the transcriptional site of STAT2 on PFKFB4 promoter. Subsequently, compared to shNC or pcDNA3.1 group, shSTAT2 transfection remarkably downregulated STAT2 and PFKFB4 expressions in NCI-H929, INA-6 and U266 cells, while pcDNA3.1-STAT2 transfection elevated STAT2 and PFKFB4 expression significantly (Fig. 5B–D, Fig. S5A–C). ChIP assay showed that PFKFB4 promoter fragments were enriched in STAT2 precipitated chromatin complex (Fig. 5E). Dual-luciferase analysis demonstrated that depletion of STAT2 suppressed the transcriptional

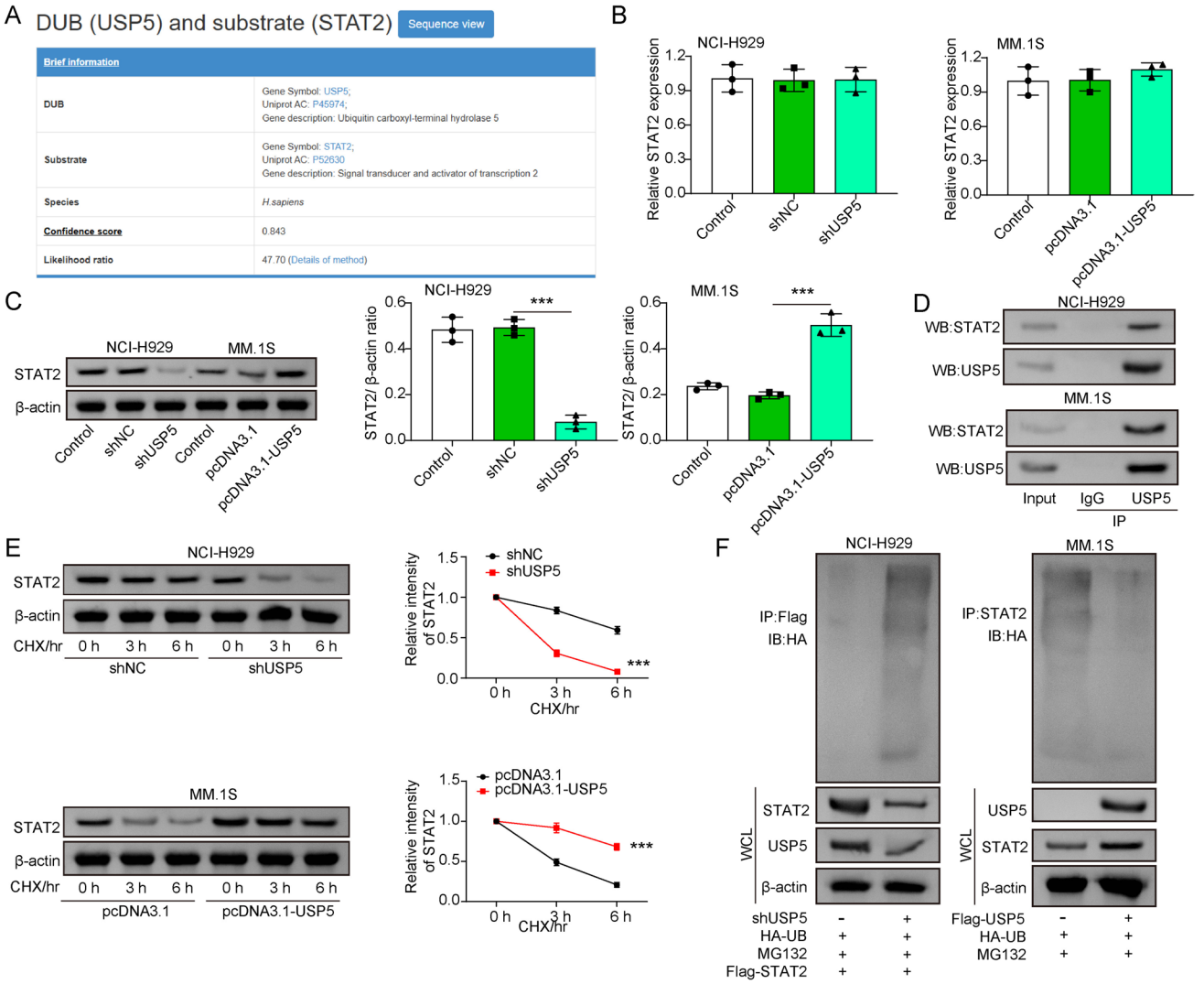

Fig. 4 USP5 stabilized STAT2 protein via promoting its deubiquitylation. **A** Schematic diagram of deubiquitylation modification site of USP5 on STAT2 predicted by Ubibrowser 2.0 database (http://ubibrowser.bio-it.cn/ubibrowser_v3/). **B**, **C** qRT-PCR and western blot were applied for measuring STAT2 expression after USP5 silence in NCI-H929 or USP5 overexpression in MM.1S cells. **D** Co-IP verified the direct interaction between USP5 and STAT2 in NCI-H929 and MM.1S cells. **E** 100 mg/L CHX was incubated with each group cells, and the degradation rate of STAT2 protein were quantified by western blot analysis. **F** In vitro ubiquitination experiment verified the ubiquitination level of STAT2. * $P<0.05$, ** $P<0.01$, *** $P<0.001$

activity of PFKFB4 in NCI-H929, INA-6 and U266 cells, but STAT2 overexpression enhanced PFKFB4 expression (Fig. 5F, Fig. S5D). Finally, STAT2 could activate PFKFB4 transcription.

USP5 facilitated the survival and glycolysis via *upregulating STAT2*

Here, we planned to probe the roles of STAT2 on USP5-mediated biological role in MM cells. At the first, STAT2 was overexpressed in NCI-H929, INA-6 and U266 cells following pcDNA3.1-STAT2 transfection, and silenced in MM.1S cells by transfection shSTAT2 (Fig. 6A, Fig. S6A). Then, functional assays demonstrated that the inhibitory role of USP5 silence on cell viability and the induction on cell apoptosis in NCI-H929, INA-6 and U266 cells were reversed after STAT2 overexpression, oppositely, the promoting impact of USP5 increase on cell viability and repressive effect on apoptosis in MM.1S cells were also diminished greatly by STAT2 (Fig. 6B, C, Fig. S6B, C). Additionally, STAT2 overexpression obviously restrained the inhibitory role of UPS5 depletion on glycolysis-related genes (HK2, PFKP, PKM2) in NCI-H929, INA-6 and U266 cells, while silencing of STAT2 downregulated the promoting roles of USP5 overexpression on glycolysis-related genes (HK2, PFKP, PKM2) levels in MM.1S cells (Fig. 6D, Fig. S6D).

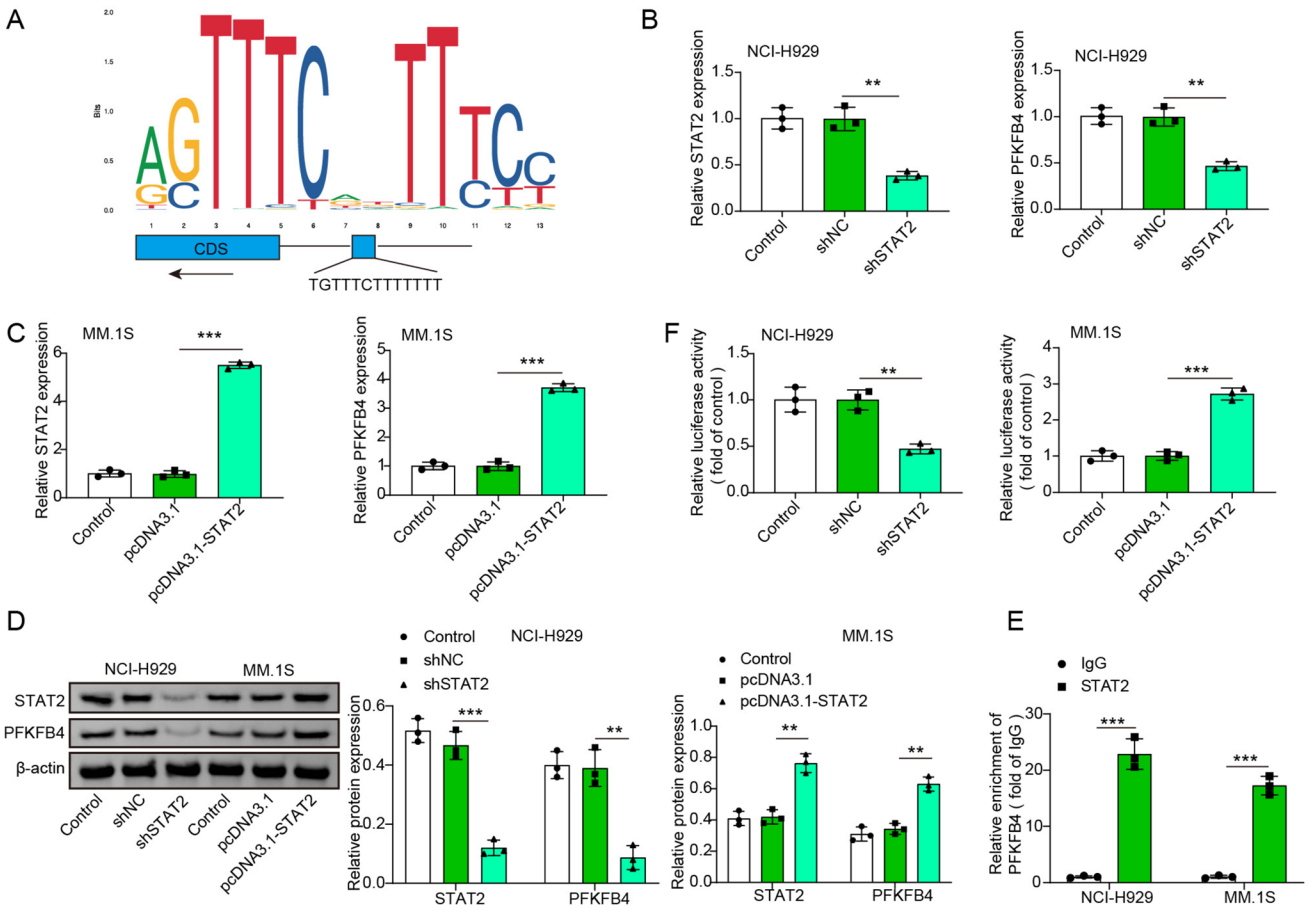

Fig. 5 USP5 activated PFKFB4 transcription. **A** Schematic diagram of transcriptional site between STAT2 and PFKFB4 predicted by JASPAR database (https://jaspar.elixir.no/). **B**, **C** qRT-PCR was conducted for identifying the mRNA level of STAT2 and PFKFB4 after shSTAT2 or pcDNA3.1-STAT2 transfection. **D** Western blot evaluated the protein levels of STAT2 and PFKFB4 after shSTAT2 or pcDNA3.1-STAT2 transfection. **E** The direct interaction between STAT2 and PFKFB4 promoter was identified by ChIP experiment. **F** The impact of STAT2 on PFKFB4 transcriptional activity was examined by dual-luciferase assay. * $P<0.05$, ** $P<0.01$, *** $P<0.001$

Consistently, the repressive effects of USP5 silencing on glucose uptake, lactate production and ATP contents were overturned by STAT2 overexpression in NCI-H929 cells, whereas STAT2 downregulation plays an opposite role in USP5-reduced MM.1S cells (Fig. 6E–G, Fig. S6E–G). In conclude, these findings observed that USP5-induced glycolysis and proliferation by increasing STAT2.

USP5-induced immunosuppressive macrophage formation by partly depending on STAT2 upregulation

The TCM from each group of MM cells was harvested separately and subsequently incubated with PBMCs-derived macrophages for 48 h. As shown in Fig. 7A–C, Fig. S7A–C, USP5 knockdown significantly repressed the characteristic levels of M2 macrophage markers (Arg1, CD206, and IL-10) as well as the rate of CD206-positive cells in NCI-H929, INA-6 and U266 cells, while USP5 overexpression enhanced these markers and the CD206-positive cell rate in MM.1S cells. However, STAT2 overexpression in NCI-H929, INA-6 and U266 cells remarkably reversed these changes mediated by USP5 depletion, and STAT2 knockdown in MM.1S cells obviously diminished the roles of USP5 overexpression (Fig. 7A–C, Fig. S7A–C). The changes of M1 macrophages exhibited a little change between each group (Fig. 7A–C, Fig. S7A–C). Overall, USP5 facilitated tumor-associated M2 macrophage polarization by regulating STAT2.

USP5 contributed to tumor growth, glycolysis and M2-like macrophage polarization in vivo

NCI-H929 cells with different treatment were mixed with macrophages at a ratio of 1:1 and injected subcutaneously into nude mice. After 4 weeks, the mice were killed, and xenografted tumor tissue was collected for further experiments. The results demonstrated that compared to control group, USP5 knockdown strikingly inhibited tumor growth,

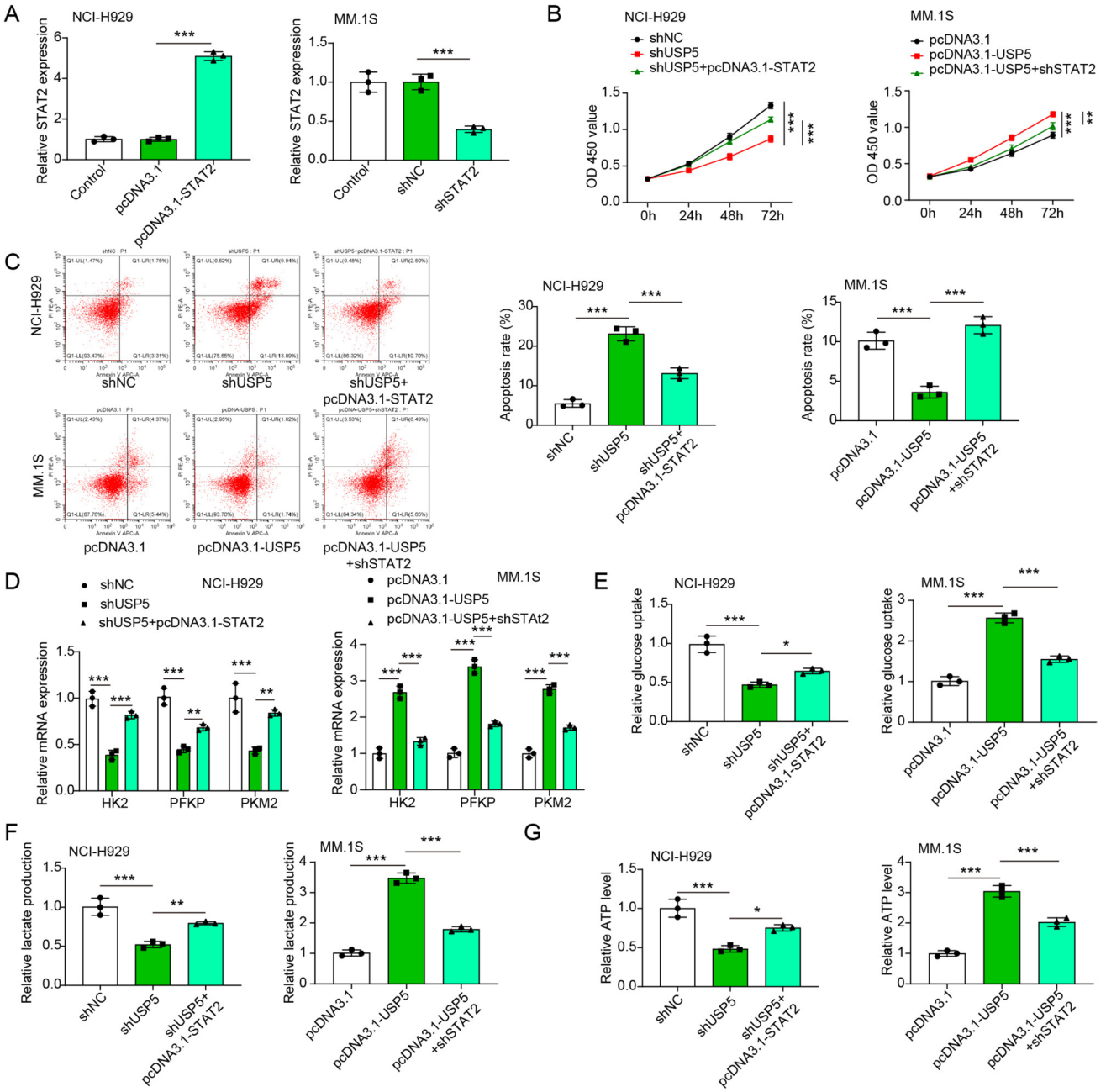

Fig. 6 USP5 facilitated the survival and glycolysis by activating STAT2. **A** qRT-PCR quantified the mRNA level of STAT2 after transfection with pcDNA3.1-STAT2 in NCI-H929 cells or shSTAT2 in MM.1S cells. NCI-H929 cells were transfected with shUSP5 alone or co-transfection with shUSP5 and pcDNA3.1-STAT2. MM.1S cells were transfected with pcDNA3.1-USP5 alone and co-transfected with pcDNA3.1-USP5 and shSTAT2. **B** CCK-8 was used to verify the cell viability. **C** Flow cytometry was utilized to determine cell apoptosis. **D** qRT-PCR was performed to identify glycolysis-related HK2, PFKP and PKM2 expressions. **E-G** The glucose uptake, lactate production and ATP level were measured by corresponding kits. * $P<0.05$, ** $P<0.01$, *** $P<0.001$

reduced tumor volume and tumor weight (Fig. 8A–C). Moreover, the mRNA and protein expressions of USP5, STAT2 and PFKFB4 were obviously downregulated in tumor tissues in shUSP5 group mice than those in control group mice (Fig. 8D–G). qRT-PCR analysis illustrated that relative control group, the levels of glycolysis-related genes (HK2, PFKP, PKM2) and M2 macrophage markers (Arg1, CD206 and IL-10) were dramatically repressed in tumor tissues from shUSP5 group mice (Fig. 8H, I). Moreover, immunofluorescence assay also displayed that USP5 knockdown remarkably decreased the co-localization of CD206 and CD11b (Fig. 8J). All these findings elucidated that USP5

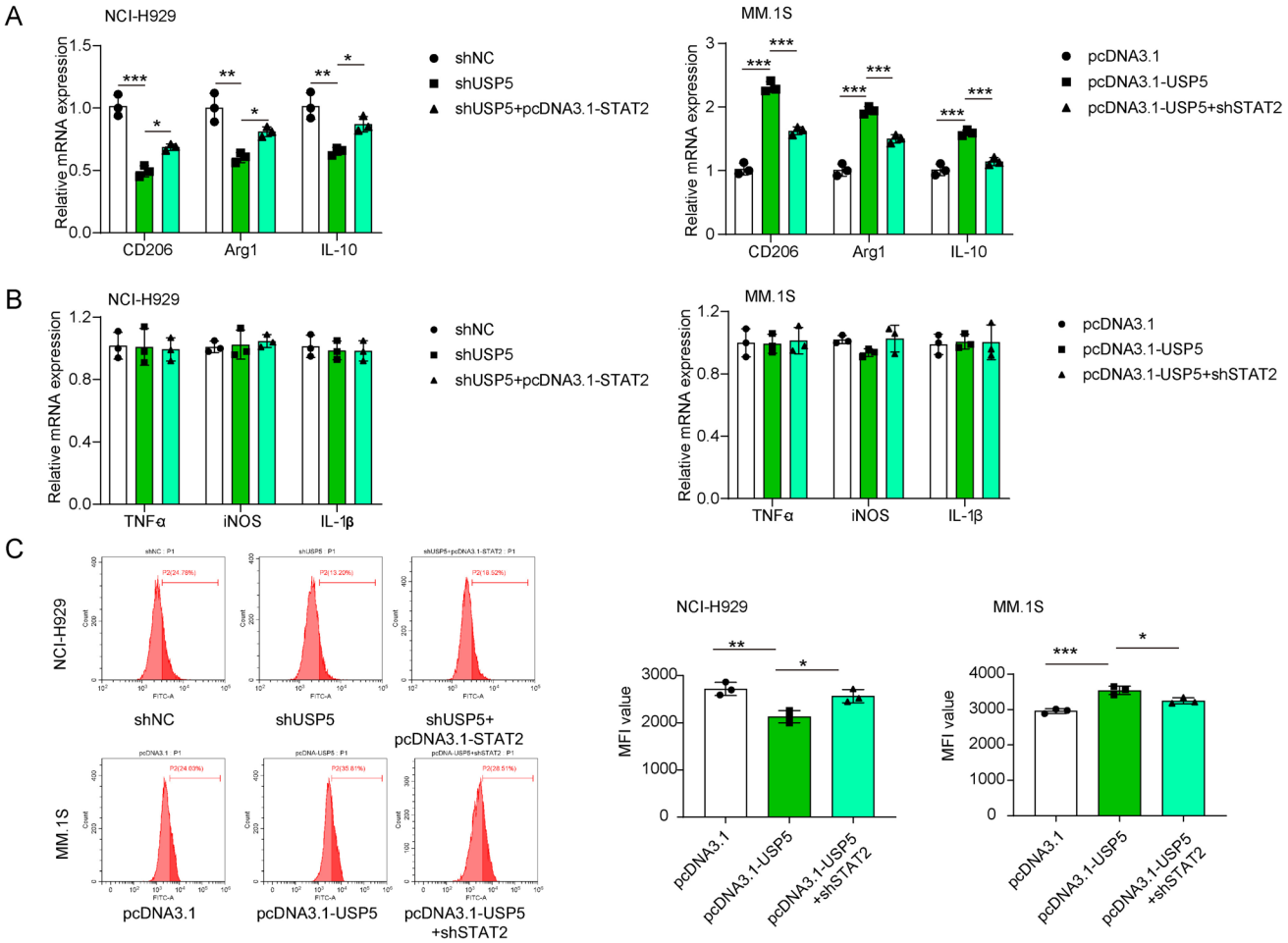

Fig. 7 USP5-induced immunosuppressive macrophage formation by partly depending on STAT2 upregulation. NCI-H929 cells were transfected with shUSP5 alone or co-transfection with shUSP5 and pcDNA3.1-STAT2. MM.1S cells were transfected with pcDNA3.1-USP5 alone and co-transfected with pcDNA3.1-USP5 and shSTAT2. Then, the TCM from each group were obtained and co-cultured with PBMCs-derived macrophages for 48 h. **A**, **B** qRT-PCR for the measurement of M1-like macrophage markers (TNF-α, iNOS, IL-1β) and M2-like macrophage markers (Arg1, CD206, IL-10). **C** Flow cytometry analysis for the assessment of CD206-positive macrophage rate. * $P<0.05$, ** $P<0.01$, *** $P<0.001$

facilitated tumor glycolysis and M2 macrophage polarization, thus contributing MM development in vivo.

Discussion

MM cells typically coordinate a microenvironment conducive to MM cell growth and metastasis by recruiting and reprogramming non-cancerous host cells and by remodeling the vascular system and extracellular matrix [12, 27, 28]. The Warburg effect is one of the most important metabolic characteristics of tumor cells, characterized by increased glucose uptake and reliance on glycolysis to convert a large amount of pyruvate into lactate [13]. Plasma cells from newly diagnosed MM patients exhibit higher rates of mitochondrial and glycolytic ATP formation, indicating that energy metabolism within plasma cells impacts the pathogenesis and outcomes of MM patients [29]. Additionally, lactate, a key product of this process, is one of the main contributors to the acidity of the tumor microenvironment and exerts immunosuppressive functions through various mechanisms. TAMs are a critical population of immune cells within the tumor microenvironment and can be classified into M1 pro-inflammatory and M2 anti-inflammatory types. Studies have shown that lactate derived from tumor cells can induce the VEGF/Arg1 pathway through the HIF-1α signaling pathway, promoting TAM polarization toward the M2 phenotype, which aids in TAM-mediated tumor growth [30]. In breast cancer, ZEB1 induces lactate formation by activating glycolysis and promotes the M2 macrophage phenotype through the PKA/CREB signaling pathway [16]. This reveals that the activated glycolysis-lactate pathway in MM

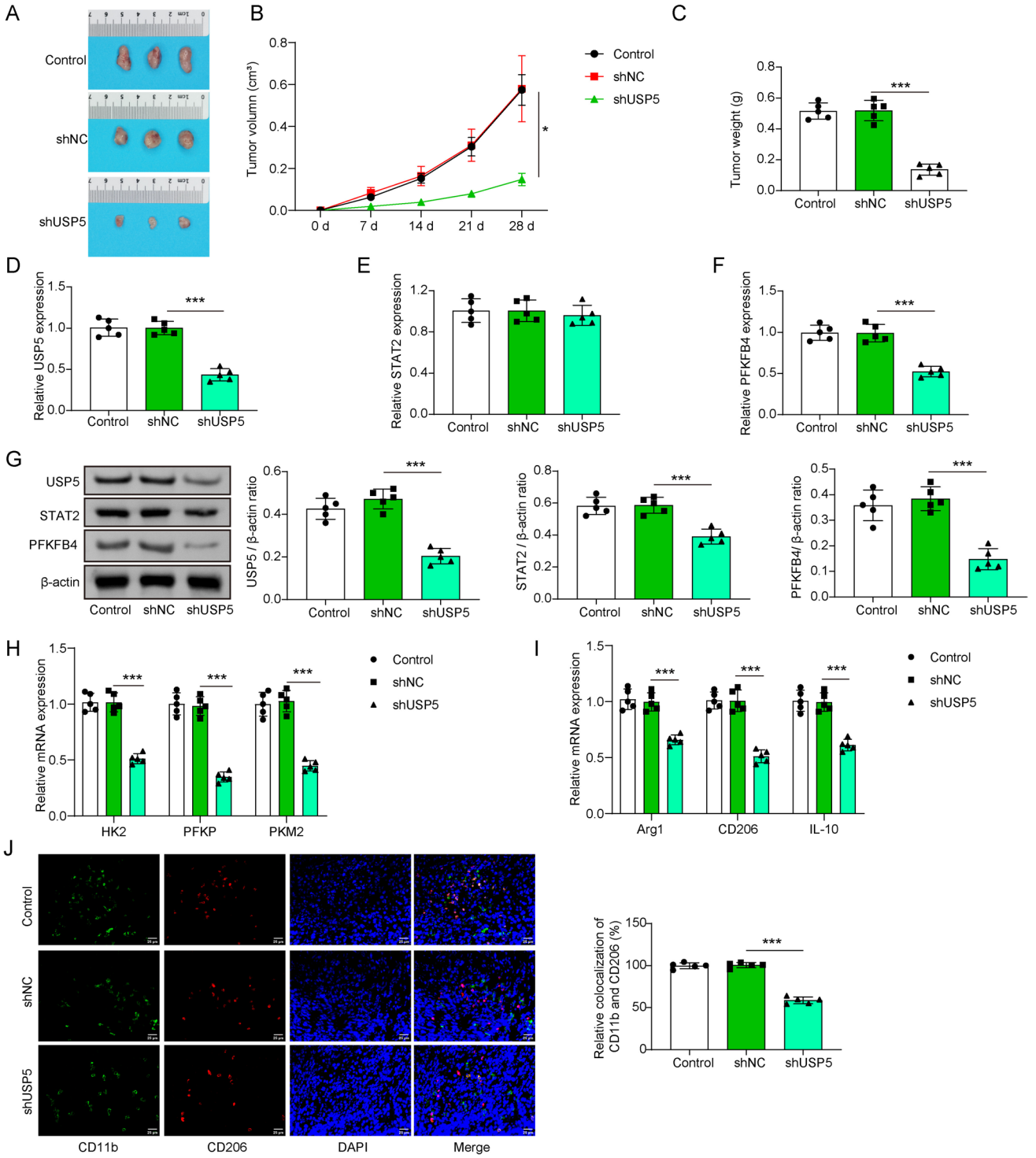

Fig. 8 USP5 contributed to tumor growth, glycolysis and M2-like macrophage polarization in vivo. NCI-H929 cells stably expressed shNC or shUSP5 were mixed with PBMCs-derived macrophages at a ratio of 1:1, and then subcutaneous injected into mice. After 4 weeks, mice were killed and the tumor tissues were collected for next detection. **A** Representative images of tumor tissues. **B** Analysis of tumor volume. **C** Data of tumor weight. **D**–**F** qRT-PCR analysis for determining USP5, STAT2 and PFKFB4. **G** Western blot for verifying the protein levels of USP5, STAT2 and PFKFB4. **H** qRT-PCR analysis for evaluated glycolysis-associated genes including HK2, PFKP and PKM2. **I** qRT-PCR analysis for assessing the markers of M2-like macrophages including Arg1, IL-10 and CD206. **J** Representative image of immunofluorescence for determining the co-location of CD206 and CD11b. * $P<0.05$, ** $P<0.01$, *** $P<0.001$

cells is crucial for inducing the formation of immunosuppressive M2 macrophages.

USP5 is a ubiquitously expressed deubiquitinating enzyme that participates in various physiological processes by removing ubiquitin modifications from target protein chains. Currently, USP5 has been identified as involved in the progression of various human cancers. For example, conditional knockout of USP5 enhances the antitumor efficacy of Trametinib or anti-CTLA-4 by promoting PD-L1 protein ubiquitination [31]. Additionally, USP5 activates the expression of downstream glycolysis-related genes (LDH-A, ENO1, TPI1, SLC2A1, and PKM2) by inhibiting K48-linked polyubiquitination of c-Myc, driving glucose metabolic reprogramming and metastasis in hepatocellular carcinoma [24]. Inhibition of USP5 protein induces apoptosis of MM cells by reducing c-Maf stability, enhancing MM sensitivity to thiabendazole [20, 22]. This further suggests the potential value of USP5 as a novel therapeutic target for cancer. Here, we have revealed high expression of USP5 in clinical samples and cell lines of MM. By establishing USP5 overexpression in the MM.1S cell line and silencing USP5 in the NCI-H929, U266 and INA-6 cell lines, we demonstrated for the first time that USP5 effectively promoted MM cell proliferation and metastasis, glycolysis, and lactate formation, corroborating the findings of Peng et al. [23]. Through co-culture experiments, we found that overexpression of USP5 significantly induced M2 macrophage polarization, a process that could be reversed by co-treatment with OXM. This discovery provided the first evidence of the critical role of the glycolysis-lactate pathway in USP5-induced immunosuppressive M2 macrophage formation in MM.

STAT2 is a member of the STAT family, participating in tumor metabolism, immunity, and tumor development by influencing gene transcription [32, 33]. Previous studies have shown that the stability of STAT2 protein is associated with CRL3-mediated E3 ubiquitin ligase modification [34], and deubiquitination catalyzed by USP18 [35], suggesting that the stability of STAT2 protein is closely related to its ubiquitination level. In this study, we reported for the first time the molecular mechanism by which USP5 reduced the ubiquitination level of STAT2 protein, thereby decreasing its stability. Traditionally, STAT2 is associated with the canonical JAK/STAT pathway and is involved in various biological processes, including the remodeling of the tumor microenvironment and antitumor immunity [36]. In MM, tyrphostin AG490 (a specific JAK2 inhibitor) induces MM cell apoptosis by blocking the MAPK and STAT signaling pathways [37]. Furthermore, STAT1/2 can activate the glycolytic pathway by increasing the expression of IFN-I genes [38, 39]. Consistent with previous research, our experimental results indicated that STAT2 exhibited oncogenic functions in MM cells by enhancing MM cell proliferation and glycolytic capacities, increasing lactate production, and inducing the differentiation of immunosuppressive M2 macrophages. This finding enriched the understanding of the pathological mechanisms of STAT2 in the development of MM. Importantly, silencing STAT2 markedly reversed the biological functions of USP5 in MM cell glycolysis and the formation of immunosuppressive macrophages, suggesting that STAT2 was a direct target of USP5-mediated glycolysis, lactate production, and immunosuppressive BMME formation in MM cells.

PFKFB4, a key regulator of glycolysis, plays a central role in controlling the glycolytic process. PFKFB4 can catalyze the conversion of fructose-6-phosphate (F-6-P) into fructose-2,6-bisphosphate (F-2,6-BP), which activates the rate-limiting enzyme in glycolysis, 6-phosphofructokinase-1 (PFK-1). Additionally, PFKFB4 catalyzes the hydrolysis of F-2,6-BP back to F-6-P, redirecting glucose energy toward the pentose phosphate pathway (PPP), producing ribose-5-phosphate and regenerating NADPH to reduce oxidative stress in tumor cells [40]. Previous literature has revealed that PFKFB4 expression is increased in various human tumors [41–43], and closely associated with tumor growth, metastasis, stemness, tumor immune suppression, and remodeling of the tumor microenvironment [40, 44, 45]. For example, PIM2 enhances glycolysis and cell growth, worsening endometriosis by phosphorylating PFKFB4 [46]. Knocking down PFKFB4 expression represses the invasive capability of breast cancer cells by decreasing lactate level [47]. In liver cancer, patients with high PFKFB4 expression exhibit an immunosuppressive microenvironment characterized by extensive infiltration of M2-like macrophages [48]. Specific inhibition of PFKFB4 decreases MM cells growth [49]. These studies confirm that PFKFB4 is a key regulatory factor in the glycolysis-lactate pathway in tumor cells. Interestingly, in this study, we provided for the first time that STAT2 activated the transcription of PFKFB4 by directly binding to its promoter, indicating that PFKFB4 was a direct effector of the USP5/STAT2 signaling axis involved in regulating glycolysis and lactate production in MM cells.

In conclusion, our research findings revealed that USP5 stabilized STAT2 protein, thereby activating PFKFB4 transcription, which endowed MM cells with aberrantly enhanced glycolysis and lactate production, leading to the formation of immunosuppressive M2 macrophages. This discovery provided new insights into the development of MM and the formation of its associated microenvironment, offering a theoretical basis for developing new anti-MM strategies.

Supplementary Information The online version contains supplementary material available at https://doi.org/10.1007/s00262-025-04031-1.

Acknowledgements We would like to give our sincere gratitude to the reviewers for their constructive comments.

Author contributions S.L. designed the study. S.L., T.D. and Y.Z. performed the experiments. S.L., T.D., J.S., Y.L. and Q.W. analyzed the data. All authors were involved in drafting and revising the manuscript.

Funding None.

Data availability All data generated or analyzed are included in this article. Further inquiries can be directed to the corresponding author.

Declarations

Conflict of interest The authors declare that they have no conflict of interest.
The authors declare no competing interests.

Ethics approval and consent to participate The collection and use of clinical specimens were approved by the ethics committee of The Affiliated Hospital of Jinggangshan University and performed in accordance with the Declaration of Helsinki. All subjects were provided written informed consent.

The animal experiment was approved by the Animal Ethics Committee of The Affiliated Hospital of Jinggangshan University. All the animal procedures were performed in accordance with the ARRIVE guidelines.

Consent for publication Not applicable.

References

1. Zhou L et al (2021) Measuring the global, regional, and national burden of multiple myeloma from 1990 to 2019. BMC Cancer 21(1):606
2. Malard F et al (2024) Multiple myeloma. Nat Rev Dis Primers 10(1):45
3. Ho M et al (2022) Treating multiple myeloma in the context of the bone marrow microenvironment. Curr Oncol 29(11):8975–9005
4. Minnie SA, Hill GR (2020) Immunotherapy of multiple myeloma. J Clin Invest 130(4):1565–1575
5. Lopes R et al (2022) Multiple myeloma-derived extracellular vesicles modulate the bone marrow immune microenvironment. Front Immunol 13:909880
6. García-Ortiz A et al (2021) The role of tumor microenvironment in multiple myeloma development and progression. Cancers 13(2):217
7. Walters DK, Arendt BK, Jelinek DF (2013) CD147 regulates the expression of MCT1 and lactate export in multiple myeloma cells. Cell Cycle 12(19):3175–3183
8. Chelakkot C et al (2023) Modulating glycolysis to improve cancer therapy. Int J Mol Sci 24(3):2606
9. Yang J et al (2020) The enhancement of glycolysis regulates pancreatic cancer metastasis. Cell Mol Life Sci 77(2):305–321
10. Raimondi V et al (2022) Metabolic features of myeloma cells in the context of bone microenvironment: Implication for the pathophysiology and clinic of myeloma bone disease. Front Oncol 12:1015402
11. El Arfani C et al (2018) Metabolic features of multiple myeloma. Int J Mol Sci 19(4):1200
12. Wu S et al (2020) Metabolic reprogramming induces immune cell dysfunction in the tumor microenvironment of multiple myeloma. Front Oncol 10:591342
13. Gao Y et al (2022) Tumor microenvironment: lactic acid promotes tumor development. J Immunol Res 2022:3119375
14. Wang JX et al (2020) Lactic acid and an acidic tumor microenvironment suppress anticancer immunity. Int J Mol Sci 21:8363
15. Colegio OR et al (2014) Functional polarization of tumour-associated macrophages by tumour-derived lactic acid. Nature 513(7519):559–563
16. Jiang H et al (2022) Zeb1-induced metabolic reprogramming of glycolysis is essential for macrophage polarization in breast cancer. Cell Death Dis 13(3):206
17. Mu X et al (2018) Tumor-derived lactate induces M2 macrophage polarization via the activation of the ERK/STAT3 signaling pathway in breast cancer. Cell Cycle 17(4):428–438
18. Wang K, Zhang Y, Chen ZN (2023) Metabolic interaction: tumor-derived lactate inhibiting CD8(+) T cell cytotoxicity in a novel route. Signal Transduct Target Ther 8(1):52
19. Yan B et al (2023) A pan-cancer analysis of the role of USP5 in human cancers. Sci Rep 13(1):8972
20. Wang S et al (2017) Inhibition of the deubiquitinase USP5 leads to c-Maf protein degradation and myeloma cell apoptosis. Cell Death Dis 8(9):e3058
21. Wu L et al (2020) miR-125a suppresses malignancy of multiple myeloma by reducing the deubiquitinase USP5. J Cell Biochem 121(1):642–650
22. Chen XH et al (2019) Mebendazole elicits potent antimyeloma activity by inhibiting the USP5/c-Maf axis. Acta Pharmacol Sin 40(12):1568–1577
23. Peng ZM et al (2024) PFKP deubiquitination and stabilization by USP5 activate aerobic glycolysis to promote triple-negative breast cancer progression. Breast Cancer Res 26(1):10
24. Xia P et al (2023) METTL5 stabilizes c-Myc by facilitating USP5 translation to reprogram glucose metabolism and promote hepatocellular carcinoma progression. Cancer Commun 43(3):338–364
25. Crawford LJ et al (2016) Identification of the APC/C co-factor FZR1 as a novel therapeutic target for multiple myeloma. Oncotarget 7(43):70481–70493
26. Zhang L, Li S (2020) Lactic acid promotes macrophage polarization through MCT-HIF1α signaling in gastric cancer. Exp Cell Res 388(2):111846
27. Layer P, Hotz J, Goebell H (1986) Stimulatory effect of hypercalcemia on pancreatic secretion is prevented by pretreatment with cholecystokinin and cholinergic agonists. Pancreas 1(6):478–482
28. Janker L et al (2019) Metabolic, anti-apoptotic and immune evasion strategies of primary human myeloma cells indicate adaptations to hypoxia. Mol Cell Proteomics 18(5):936–953
29. Evans LA et al (2022) Overexpression of the energy metabolism transcriptome within clonal plasma cells is associated with the pathogenesis and outcomes of patients with multiple myeloma. Am J Hematol 97(7):895–902
30. Zhao P et al (2023) Targeting lactate metabolism and immune interaction in breast tumor via protease-triggered delivery. J Control Release 358:706–717

31. Xiao X et al (2023) ERK and USP5 govern PD-1 homeostasis via deubiquitination to modulate tumor immunotherapy. Nat Commun 14(1):2859
32. Wang Z et al (2022) The Fibrillin-1/VEGFR2/STAT2 signaling axis promotes chemoresistance via modulating glycolysis and angiogenesis in ovarian cancer organoids and cells. Cancer Commun 42(3):245–265
33. Yang Y et al (2023) circCAPRIN1 interacts with STAT2 to promote tumor progression and lipid synthesis via upregulating ACC1 expression in colorectal cancer. Cancer Commun 43(1):100–122
34. Ren W et al (2024) Zika virus NS5 protein inhibits type I interferon signaling via CRL3 E3 ubiquitin ligase-mediated degradation of STAT2. Proc Natl Acad Sci U S A 121(34):e2403235121
35. Espada CE et al (2024) ISG15/USP18/STAT2 is a molecular hub regulating IFN I-mediated control of Dengue and Zika virus replication. Front Immunol 15:1331731
36. Canar J et al (2023) The duality of STAT2 mediated type I interferon signaling in the tumor microenvironment and chemoresistance. Cytokine 161:156081
37. De Vos J et al (2000) JAK2 tyrosine kinase inhibitor tyrphostin AG490 downregulates the mitogen-activated protein kinase (MAPK) and signal transducer and activator of transcription (STAT) pathways and induces apoptosis in myeloma cells. Br J Haematol 109(4):823–828
38. Vandsemb EN et al (2021) PRL-3 induces a positive signaling circuit between glycolysis and activation of STAT1/2. Febs j 288(23):6700–6715
39. Smith CN, Blackburn JS (2021) PRL-3 promotes a positive feedback loop between STAT1/2-induced gene expression and glycolysis in multiple myeloma. Febs j 288(23):6674–6676
40. Dai T et al (2022) Hypoxic activation of PFKFB4 in breast tumor microenvironment shapes metabolic and cellular plasticity to accentuate metastatic competence. Cell Rep 41(10):111756
41. Wang W, Wang B (2022) KDM3A-mediated SP1 activates PFKFB4 transcription to promote aerobic glycolysis in osteosarcoma and augment tumor development. BMC Cancer 22(1):562
42. Wu Y et al (2022) Loss of PFKFB4 induces cell cycle arrest and glucose metabolism inhibition by inactivating MEK/ERK/c-Myc pathway in cervical cancer cells. J Obstet Gynaecol 42(6):2399–2405
43. Lu H et al (2020) PFKFB4 negatively regulated the expression of histone acetyltransferase GCN5 to mediate the tumorigenesis of thyroid cancer. Dev Growth Differ 62(2):129–138
44. Gu X et al (2023) Differential roles of highly expressed PFKFB4 in colon adenocarcinoma patients. Sci Rep 13(1):16284
45. Zhou Y et al (2022) Effect of PFKFB4 on the Prognosis and Immune Regulation of NSCLC and Its Mechanism. Int J Gen Med 15:6341–6353
46. Lu C et al (2022) Phosphorylation of PFKFB4 by PIM2 promotes anaerobic glycolysis and cell proliferation in endometriosis. Cell Death Dis 13(9):790
47. Kar S et al (2023) Reprogramming of glucose metabolism via PFKFB4 is critical in FGF16-driven invasion of breast cancer cells. Biosci Rep. https://doi.org/10.1042/BSR20230677
48. Gu Y et al (2024) Immune- and metabolism-related gene signature analysis uncovers the prognostic and immune microenvironments of hepatocellular carcinoma. J Cancer Res Clin Oncol 150(6):311
49. Okabe S, Tanaka Y, Gotoh A (2022) Therapeutic targeting of PFKFB3 and PFKFB4 in multiple myeloma cells under hypoxic conditions. Biomark Res 10(1):31